

Flow Augmentation and Knowledge Distillation for Lightweight Face Presentation Attack Detection

Muhammad Shahid Jabbar¹, Muhammad Sohail Ibrahim², Taha Hasan Masood Siddique³,
Kejie Huang³ and Shujaat Khan^{1,4}

¹ SDAIA-KFUPM Joint Research Center for Artificial Intelligence, King Fahd University of Petroleum & Minerals, Dhahran, Saudi Arabia

² Interdisciplinary Research Center for Intelligent Secure Systems (IRC-ISS), King Fahd University of Petroleum & Minerals, Dhahran, Saudi Arabia

³ College of Information Science & Electronic Engineering, Zhejiang University, Hangzhou, China

⁴ Department of Computer Engineering, College of Computing and Mathematics, King Fahd University of Petroleum & Minerals, Dhahran, Saudi Arabia

Abstract—Face presentation attack detection (FacePAD) remains challenging under diverse spoofing representation, including 2D print and replay, 3D mask-based spoofing, makeup-induced appearance manipulation, and physical occlusions, as well as under varying capture conditions. Motion cues are highly discriminative for FacePAD but typically require explicit optical flow estimation, which introduces substantial computational overhead and limits real-time deployment. In this work, we leverage optical flow to enhance motion representation during training while eliminating the need for flow computation at inference. We propose a dual-branch teacher model that fuses appearance cues from RGB frames with motion cues derived from colorwheel-encoded optical flow, enabling effective modeling of micro-motions and temporal consistency. To enable efficient deployment, we introduce a knowledge distillation framework that transfers motion-aware knowledge from the flow-augmented teacher to a lightweight RGB-only student via logit distillation. As a result, the student implicitly learns motion-sensitive representations without requiring explicit flow estimation or additional feature extraction blocks at inference. Extensive experiments demonstrate strong performance across multiple benchmarks, achieving 0.0% HTER on Replay-Attack and Replay-Mobile, 0.94% HTER on ROSE-Youtu, 5.65% HTER on SiW-Mv2, and 0.42% ACER on OULU-NPU. The distilled student achieves performance comparable to or better than the teacher while significantly reducing parameters and FLOPs, achieving 52 FPS on an NVIDIA@Jetson Orin Nano, indicating its suitability for real-time and resource-constrained FacePAD deployment.

I. INTRODUCTION

Face recognition systems are widely deployed in biometric applications such as smartphone authentication, surveillance, mobile payments, and access control, yet they remain vulnerable to presentation attacks (PAs) including printed photos, replayed videos, and 2D/3D masks. Face presentation attack detection (FacePAD), also known as face anti-spoofing, aims to distinguish bonafide users from spoofing attempts [1].

Early FacePAD methods rely on handcrafted features and classical machine learning, however, such techniques suffered from limited robustness to variations in illumination, camera quality, and capture conditions [1]. With the advent of deep learning, CNN-based approaches have become dominant, achieving improved generalization using learned appearance representations [2], [3], [4]. To further enhance

liveness detection, auxiliary cues have been explored, including physiological signals [5] and depth supervision [6], [7]. However, such approaches often incur high computational cost or remain susceptible to sophisticated spoofing artifacts.

Motion information has emerged as a particularly effective cue for FacePAD, as genuine faces exhibit non-rigid temporal dynamics that are difficult to reproduce using spoofing media. Optical flow provides a principled representation of such motion by modeling pixel-level displacement across frames. Early works exploit differences between planar and non-planar motion fields for liveness detection [8], [9], while recent approaches incorporate handcrafted or learned flow-based descriptors to capture temporal dynamics [10], [11]. More recent deep models integrate optical flow with appearance cues using attention mechanisms or deep dynamic texture representations to better model fine-grained facial motion [12], [13], [14]. Despite their effectiveness, such methods typically require explicit optical flow estimation and additional feature extraction blocks, leading to increased inference latency and memory overhead that limit real-time and resource-constrained deployment.

To overcome these limitations, we propose a knowledge distillation framework that leverages motion cues during training while eliminating explicit optical flow computation at inference. A motion-aware teacher model incorporates a dedicated optical flow branch to guide the learning of robust liveness representations, and transfers this knowledge to a lightweight RGB-only student model via logit-based knowledge distillation. The key contributions of this work are summarized as follows:

- We propose a dual-branch FacePAD teacher architecture that fuses RGB appearance cues with colorwheel-encoded optical flow to capture micro-motions and temporal consistency.
- We exploit consecutive video frames ($\Delta t = 1$) to enhance motion cues without introducing additional sensing modalities.
- We introduce a logit-based knowledge distillation strategy that enables a lightweight RGB-only student to implicitly

learn motion-sensitive representations, removing the need for explicit optical flow estimation at inference.

- Extensive experiments demonstrate that the distilled student achieves competitive performance with significantly reduced computational complexity, enabling efficient real-time FacePAD deployment.

II. PROPOSED METHOD

A. Frame Sampling and Flow Estimation

The input consists of RGB video frames. From each clip, a reference frame at time t ,

$$X_t^{(i)} \in \mathbb{R}^{3 \times H \times W},$$

is sampled, where i indexes the clip. During training, t is chosen randomly to promote variability; at inference, the first frame is used. To extract motion cues, a temporally adjacent frame at $t + \Delta t$ (where $\Delta t = 1$),

$$X_{t+\Delta t}^{(i)} \in \mathbb{R}^{3 \times H \times W},$$

is paired with $X_t^{(i)}$, and optical flow is estimated on-the-fly:

$$\mathbf{U}_{t,t+\Delta t}^{(i)} = (u, v) \leftarrow \text{FlowEngine}(X_t^{(i)}, X_{t+\Delta t}^{(i)}) \in \mathbb{R}^{2 \times H \times W}.$$

Flow estimation. The FlowEngine is instantiated with the *UniMatch* network [15], using the MixData-pretrained checkpoint and standard hyperparameters (multi-scale transformer encoder, iterative refinement, and windowed attention). To match the training distribution of UniMatch, inputs are scaled to the 0–255 range if originally in $[0, 1]$, transposed if necessary to ensure width \geq height, and bilinearly resized to multiples of 32. The resulting flow field $\mathbf{U}_{t,t+\Delta t}^{(i)}$ is resized back to the original resolution with magnitude correction, and any transposition is reversed. The estimator outputs pixel-wise displacements in *pixel units*, aligned with the original grid.

Pre-processing and augmentation. The 2-channel flow field $\mathbf{U}_{t,t+\Delta t}^{(i)}$ is encoded into a 3-channel image via HSV-to-RGB colorwheel mapping,

$$X_{\text{FLOW},t}^{(i)} \in \mathbb{R}^{3 \times H \times W},$$

for compatibility with CNN backbones. Identical geometric operations are then applied to both modalities: (i) adaptive center cropping to the largest square region, and (ii) resizing to $\rho \times \rho$ with $\rho = 224$. When resizing flow, vector magnitudes are scaled to preserve physical consistency. During training, synchronized random augmentations (in-plane rotation, isotropic scaling) are applied with shared parameters to maintain alignment between $X_t^{(i)}$ and $\mathbf{U}_{t,t+\Delta t}^{(i)}$. At inference, only deterministic cropping and resizing are used.

For knowledge distillation, the student model follows the same preprocessing pipeline but requires only RGB frames, eliminating dependence on the flow estimator at inference.

B. Network Architecture

The proposed approach couples appearance and motion cues through a dual-branch teacher network fed by an RGB frame and a colorwheel-encoded flow image computed from an adjacent frame (Algorithm 1; Fig. 1). After preprocessing, each sample provides $\tilde{X}_{\text{RGB}}^{(i)} \in \mathbb{R}^{3 \times \rho \times \rho}$ and $\tilde{X}_{\text{FLOW}}^{(i)} \in \mathbb{R}^{3 \times \rho \times \rho}$.

Algorithm 1: FacePAD teacher model with flow augmentation

Input: Batch of video sequences $V \in \mathbb{R}^{B \times 3 \times H \times W}$

Output: Class predictions $Y \in \mathbb{R}^{B \times 2}$

Given:

FlowEngine: optical flow estimator;

Colorwheel: mapping flow (u, v) to RGB via HSV;

SyncAug: synchronized transforms for RGB and Flow;

CNN_{RGB}, CNN_{FLOW}: encoders;

FC: classifier head;

Temporal offset: $\Delta t = 1$

- 1 Initialize an empty list $Y = []$.
 - 2 **for** each sample $i = 1, \dots, B$ **do**
 - 3 Reference frame: $X_t^{(i)} \leftarrow V[i]$.
 - 4 Adjacent frame: $X_{t+\Delta t}^{(i)}$.
 - 5 Flow: $\mathbf{U}_{t,t+\Delta t}^{(i)} \leftarrow \text{FlowEngine}(X_t^{(i)}, X_{t+\Delta t}^{(i)})$.
 - 6 Encode as RGB: $X_{\text{FLOW},t}^{(i)} \leftarrow \text{Colorwheel}(\mathbf{U}_{t,t+\Delta t}^{(i)})$.
 - 7 Preprocess:
 $(\tilde{X}_{\text{RGB}}^{(i)}, \tilde{X}_{\text{FLOW}}^{(i)}) \leftarrow \text{SyncAug}(X_t^{(i)}, X_{\text{FLOW},t}^{(i)})$.
 - 8 Features:
 - 9 $\mathbf{f}_{\text{RGB}}^{(i)} \leftarrow \text{CNN}_{\text{RGB}}(\tilde{X}_{\text{RGB}}^{(i)})$,
 - 10 $\mathbf{f}_{\text{FLOW}}^{(i)} \leftarrow \text{CNN}_{\text{FLOW}}(\tilde{X}_{\text{FLOW}}^{(i)})$.
 - 11 Concatenate: $\mathbf{f}^{(i)} \leftarrow [\mathbf{f}_{\text{RGB}}^{(i)}, \mathbf{f}_{\text{FLOW}}^{(i)}]$.
 - 12 Predict: $y^{(i)} \leftarrow \text{FC}(\mathbf{f}^{(i)})$; append to Y .
 - 13 **end**
 - 14 **return** Predictions Y
-

Two ImageNet-pretrained MobileNetV3-Large backbones encode RGB and flow inputs independently. MobileNetV3-Large backbones are used for its favorable performance–efficiency trade-off, which is critical for real-time FacePAD deployment on edge and embedded platforms [7], [16], [17], [18].

$$\mathbf{f}_{\text{RGB}}^{(i)} = \text{CNN}_{\text{RGB}}(\tilde{X}_{\text{RGB}}^{(i)}), \quad \mathbf{f}_{\text{FLOW}}^{(i)} = \text{CNN}_{\text{FLOW}}(\tilde{X}_{\text{FLOW}}^{(i)}).$$

The flow branch processes the 3-channel colorwheel-encoded image, implicitly capturing motion direction and magnitude. Late fusion concatenates features,

$$\mathbf{f}^{(i)} = [\mathbf{f}_{\text{RGB}}^{(i)}, \mathbf{f}_{\text{FLOW}}^{(i)}],$$

followed by an MLP classifier producing logits $\mathbf{s}^{(i)} \in \mathbb{R}^2$ and posterior scores $\hat{\mathbf{p}}^{(i)} = \text{softmax}(\mathbf{s}^{(i)})$.

Knowledge distillation. We distill the dual-branch teacher into a single-branch MobileNetV3-Large student operating on RGB only. The student is trained with a combined objective:

$$\mathcal{L} = (1 - \alpha) \text{CE}(y, s_S) + \alpha T^2 \text{KL}(\text{softmax}(\frac{s_T}{T}) \parallel \text{softmax}(\frac{s_S}{T})),$$

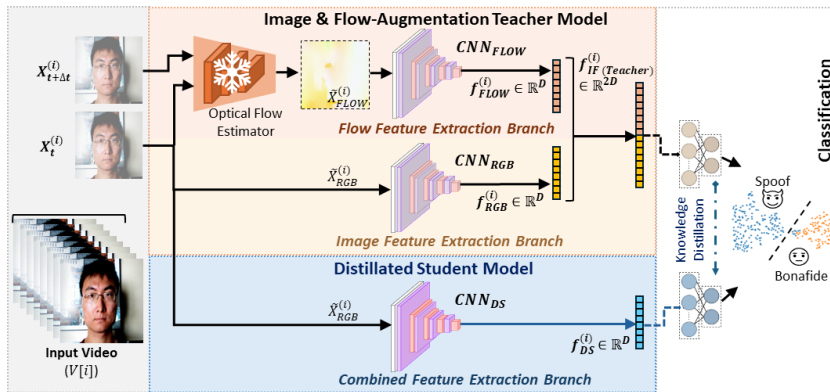


Fig. 1: Proposed dual-branch (RGB+Flow) teacher and distilled RGB-only student for FacePAD.

where CE is the cross-entropy between student logits s_S and ground-truth label y , KL matches softened distributions of teacher and student logits, T is the temperature, and α balances the terms. This eliminates reliance on flow estimation at inference while retaining competitive performance.

C. Performance Metrics

We report both *classification* and *computational* metrics. Classification metrics include Accuracy, AUC-ROC, and Half Total Error Rate (HTER). HTER is defined as $\text{HTER} = (\text{FAR} + \text{FRR})/2$, with $\text{FAR} = \text{FP}/(\text{FP} + \text{TN})$ and $\text{FRR} = \text{FN}/(\text{FN} + \text{TP})$, where TP , TN , FP , and FN denote true/false positives and negatives.

AUC-ROC is computed by threshold sweeping. We report Equal Error Rate (EER), defined at the threshold where $\text{FAR} = \text{FRR}$, and the Youden index $\max(\text{TPR} - \text{FPR})$ as a complementary summary. We also report attack classification error rate (ACER), defined as $\text{ACER} = \frac{\text{APCER} + \text{BPCER}}{2}$, where APCER and BPCER are defined as attack presentation classification error rate and bonafide presentation classification error rate, respectively.

Computational efficiency is reported with model size (parameters) and FLOPs per $\rho \times \rho$ input to compare the dual-branch teacher and distilled student, along with deployment throughput (fps) for the student model.

D. Implementation Details

The flow-augmented teacher is trained using Adam ($\text{lr}=10^{-4}$) with cross-entropy loss, batch size 16, for up to 100 epochs, with an early stopping patience of 20 epochs. Testing is performed with batch size 256. Optical flow is computed *on-the-fly* using UniMatch (Section II-A) with the temporal offset of $\Delta t = 1$. The distilled student (DS) employs MobileNetV3-Large with RGB-only input, trained under the same optimization settings, with distillation temperature $T=3$ and balance factor $\alpha=0.7$. All experiments are conducted on a single NVIDIA RTX A4500 GPU. Three independent experimental runs are conducted, and mean results are reported.

III. EXPERIMENTS AND RESULTS

A. Datasets

We evaluate the proposed models on three widely used FacePAD benchmarks: REPLAY-ATTACK (RA) [19], REPLAY-MOBILE (RM) [20], ROSE-YOUTU (RY) [21], OULU-NPU [22], and SiW-Mv2 [23]. RA, RM, and OULU-NPU comprise bonafide and spoof attempts with print and video-replay attacks, RY additionally includes paper-mask attacks and multiple capture devices, while SiW-Mv2 includes a 14 different attacks, comprising obfuscation makeup, partial coverings, etc., making it particularly challenging. We follow the official subject-disjoint protocols. From each video clip, a single RGB reference frame is sampled along with its temporal neighbor at offset $\Delta t = 1$ for flow-based experiments. Table I summarizes dataset statistics.

TABLE I: Summary of datasets used in this study.

Dataset	Year	Subjects	Genuine / Spoof Clips
Replay-Attack [19]	2012	50	300 / 1000
Replay-Mobile [20]	2016	39	540 / 624
ROSE-Youtu [21]	2018	20	1000 / 2350
OULU-NPU [22]	2017	55	990 / 3960
SiW-Mv2 [23]	2022	600	785 / 915

B. Results

Table II reports the performance of image-only (I) and flow-augmented ($I\&F$) models. On RA and RM, the flow-augmented model as well as the image-only model achieve **perfect detection** (0.0% HTER, 100% Accuracy). On RY, augmenting RGB with flow yields significant performance gain: $I\&F$ model attains improved HTER (0.94%), AUC (0.9993), and Accuracy (98.57%). On OULU-NPU, the $I\&F$ model achieves significantly superior ACER (0.42%). Similar performance trend is observed with SiW-Mv2 dataset attaining a competitive EER (6.07%) compared to the performance of image-only model.

Knowledge distillation further compresses the model. As shown in Table III, the distilled student achieves superior performance (HTER 0.81%, AUC 0.9996, Acc. 98.86%) compared to the teacher $I\&F$ model while reducing parameters, FLOPs, and memory footprint by an order of magnitude.

TABLE II: Performance comparison of the proposed flow-augmented FacePAD method ($I\&F$) with the image-only model (I) on the benchmark datasets.

Metric \ Dataset / Method	REPLAY-ATTACK		REPLAY-MOBILE		ROSE-YOUTU		OULU-NPU		SiW-Mv2	
	I	$I\&F$	I	$I\&F$	I	$I\&F$	I	$I\&F$	I	$I\&F$
Accuracy (%)	100	100	100	100	98.06	98.57	98.89	99.78	92.30	91.81
AUC-ROC	1.000	1.000	1.000	1.000	0.999	0.9993	1.000	0.999	0.981	0.987
EER (%)	0.0	0.0	0.0	0.0	1.39	0.98	0.97	0.14	6.63	6.08
HTER (%)	0.0	0.0	0.0	0.0	1.47	0.94	0.63	0.21	6.11	5.65
FAR (%)	0.0	0.0	0.0	0.0	1.39	0.92	0.42	0.14	8.01	7.46
FRR (%)	0.0	0.0	0.0	0.0	1.56	0.97	0.83	0.28	4.21	3.83
Youden's Index	1.00	1.00	1.00	1.00	0.971	0.981	0.988	0.996	0.877	0.887
ACER (%)	-	-	-	-	-	-	1.25	0.42	-	-

TABLE III: Knowledge distillation on ROSE-YOUTU dataset: $I\&F$ teacher vs. distilled student (DS).

Metric \ Model	$I\&F$	DS (RGB-only)
Parameters (M)	14.29	3.46
GFLOPs	356.63	0.22
Model Size (MB)	54.97	13.42
Peak GPU Mem. (MB)	751	30
Accuracy (%)	98.57	98.86
AUC-ROC	0.9993	0.9996
EER (%)	0.98	1.08
HTER (%)	0.94	0.81

Furthermore, implementation of the distilled student model on NVIDIA®Jetson Orin Nano resulted in a frame rate, measured in frames per second (FPS), of 52 compared to an FPS of 46 on an Intel®Core™i5 10400@2.80 GHz CPU. The computational performance underscores the practicality and real-time applicability of the proposed motion-cue distillation for real-world deployment.

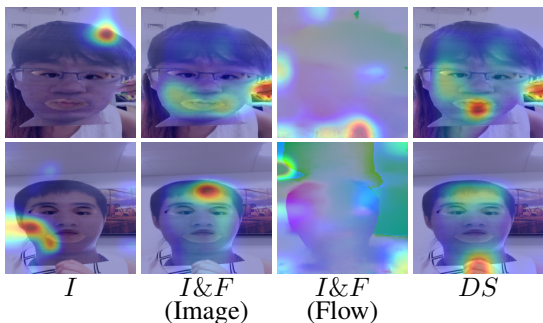


Fig. 2: Grad-CAM overlays for Image-only (I), flow-augmented ($I\&F$), and distilled student (DS) models, showing sharper motion-aware activations with flow guidance.

Grad-CAM visualizations (Fig. 2) demonstrate that flow-guided training sharpens focus on motion-consistent regions, supporting the observed performance gains.

C. Comparison with State-of-the-Art

Table IV benchmark our models against recent state-of-the-art methods. On RA and RM, both teacher and student models achieve perfect detection (0.0% HTER), matching or exceeding the best reported results. On RY, our distilled student achieves 0.81% HTER, outperforming strong baselines such as CA-FAS [24], AdvSpooGuard [17], and Depth-augmented Teacher [7] while remaining substantially more efficient. On SiW-Mv2, the proposed teacher achieves

competitive HTER/EER, while the distilled student closely matches teacher performance. Although the proposed DS model shows slightly inferior performance compared to ResNet50V2 [25] and EfficientNet-B0 [26], these methods rely on substantially larger backbones (25.6M and 5.3M parameters, respectively) compared to only 3.46M parameters for the proposed DS model.

TABLE IV: Comparison with state-of-the-art methods.

Method	Year	RA	RM	RY	SiW-Mv2
ResNet50V2 [25]	2023	0.03	0.0	2.53/2.64	5.18/6.08
EfficientNet-B0 [26]	2024	36.88	4.62	9.54/-	4.82/5.80
Spatio-Temporal ($\tau = 1$) [16]	2025	0.0	0.0	1.47/ 0.85	6.11/6.63
AdvSpooGuard [17]	2025	0.0	0.0	1.97/1.08	-
Depth-aug. Teacher [7]	2025	0.0	0.0	1.02/1.15	5.82/6.08
Depth-aug. Student [7]	2025	0.0	0.0	1.01/1.39	-
Proposed (I&F)	2026	0.0	0.0	0.94/0.98	5.65/6.07
Proposed (DS)	2026	0.0	0.0	0.81/1.08	5.78/6.35

Results are HTER (%) for RA & RM, HTER/EER (%) for RY & SiW-Mv2.

Table V presents the comparative performance on OULU-NPU dataset. The proposed methods achieve superior performance compared to the state-of-the-art methods, with the distilled student model (DS) obtaining the best performance at 0.35% ACER, followed by the proposed flow-augmented model ($I\&F$) with 0.42% ACER. These results highlight the effectiveness of the proposed method for robust and lightweight FacePAD.

TABLE V: Performance comparison of the proposed method with the state-of-the-art methods on OULU-NPU dataset.

Method	Year	APCER (%)	BPCER (%)	ACER (%)
ED-LBP (VAR) [27]	2021	11.3	8.4	9.9
Texture (VAR) [28]	2021	14.5	15	14.8
Fake-Net (VAR) [29]	2021	5.4	6.9	6.2
OFT (VAR) [14]	2022	5.7	2.7	4.2
ELA [30]	2023	-	-	4.86
3D-LCN [31]	2024	1.5	0.5	1.0
Spatio-Temporal [16]	2025	1.94	0.55	1.25
Depth-aug. Student (MB-V3) [7]	2025	1.39	0.83	1.11
Depth-aug. Student (MB-V2) [7]	2025	0.28	0.83	0.56
Proposed (I&F)	2026	0.28	0.56	0.42
Proposed (DS)	2026	0.14	0.56	0.35

VAR: Video Attack Return, OFT: Optical Flow + Texture, MB: MobileNet.

IV. CONCLUSION

This paper presents an efficient FacePAD framework that leverages motion information during training to enhance liveness modeling while avoiding the computational overhead of explicit motion estimation at inference. A dual-branch teacher network integrates appearance cues from

RGB frames with motion cues derived from colorwheel-encoded optical flow, enabling effective learning of micro-motion patterns and temporal consistency. Extensive experiments demonstrate strong performance across multiple benchmarks, achieving 0.0% HTER on Replay-Attack and Replay-Mobile, 0.94% HTER on ROSE-Youtu, 5.65% HTER on SiW-Mv2, and 0.42% ACER on OULU-NPU. To support deployment in resource-constrained and real-time scenarios, the motion-aware teacher is distilled into a lightweight RGB-only student model. The distilled student preserves motion-sensitive representations without requiring explicit flow computation and additional feature extraction at inference, attaining performance comparable to or better than the teacher while significantly reducing model complexity. Moreover, the student achieves 52 FPS on an NVIDIA® Jetson Orin Nano, demonstrating the practicality of the proposed motion-guided knowledge distillation framework for accurate, real-time, and deployable FacePAD systems.

V. ACKNOWLEDGMENTS

Taha Hasan Masood Siddique and Kejie Huang would like to acknowledge the support received from Zhejiang Province's Leading Talent Project in Science and Technology Innovation (2023R5204).

Shujaat Khan acknowledges the support of King Fahd University of Petroleum and Minerals (KFUPM) under the Early Career Grant No. EC241027.

REFERENCES

- [1] Z. Yu, Y. Qin, X. Li, C. Zhao, Z. Lei, and G. Zhao, "Deep learning for face anti-spoofing: A survey," *IEEE Transactions on Pattern Analysis and Machine Intelligence*, vol. 45, no. 5, pp. 5609–5631, 2023.
- [2] O. Lucena, A. Junior, V. Moia, R. Souza, E. Valle, and R. Lotufo, "Transfer learning using convolutional neural networks for face anti-spoofing," in *Image Analysis and Recognition: 14th International Conference, ICIAR 2017, Montreal, QC, Canada, July 5–7, 2017, Proceedings 14*. Springer, 2017, pp. 27–34.
- [3] C. Nagpal and S. R. Dubey, "A performance evaluation of convolutional neural networks for face anti spoofing," in *2019 international joint conference on neural networks (IJCNN)*. IEEE, 2019, pp. 1–8.
- [4] J. Gan, S. Li, Y. Zhai, and C. Liu, "3d convolutional neural network based on face anti-spoofing," in *2017 2nd international conference on multimedia and image processing (ICMIP)*. IEEE, 2017, pp. 1–5.
- [5] Y. Liu, A. Jourabloo, and X. Liu, "Learning deep models for face anti-spoofing: Binary or auxiliary supervision," in *Proceedings of the IEEE conference on computer vision and pattern recognition*, 2018, pp. 389–398.
- [6] Y. Atoum, Y. Liu, A. Jourabloo, and X. Liu, "Face anti-spoofing using patch and depth-based cnns," in *2017 IEEE international joint conference on biometrics (IJCB)*. IEEE, 2017, pp. 319–328.
- [7] M. S. Jabbar, T. H. M. Siddique, K. Huang, and S. Khan, "Knowledge distillation with predicted depth for robust and lightweight face presentation attack detection," *Knowledge-Based Systems*, p. 114325, 2025.
- [8] W. Bao, H. Li, N. Li, and W. Jiang, "A liveness detection method for face recognition based on optical flow field," in *2009 International Conference on Image Analysis and Signal Processing*. IEEE, 2009, pp. 233–236.
- [9] K. Kollreider, H. Fronthaler, and J. Bigun, "Non-intrusive liveness detection by face images," *Image and Vision Computing*, vol. 27, no. 3, pp. 233–244, 2009.
- [10] W. Yin, Y. Ming, and L. Tian, "A face anti-spoofing method based on optical flow field," in *2016 IEEE 13th international conference on signal processing (ICSP)*. IEEE, 2016, pp. 1333–1337.
- [11] L. Feng, L.-M. Po, Y. Li, X. Xu, F. Yuan, T. C.-H. Cheung, and K.-W. Cheung, "Integration of image quality and motion cues for face anti-spoofing: A neural network approach," *Journal of Visual Communication and Image Representation*, vol. 38, pp. 451–460, 2016.
- [12] R. Shao, X. Lan, and P. C. Yuen, "Joint discriminative learning of deep dynamic textures for 3d mask face anti-spoofing," *IEEE Transactions on Information Forensics and Security*, vol. 14, no. 4, pp. 923–938, 2018.
- [13] Z. Cheng and X. Zhang, "Integrating fine-grained classification and motion relation analysis for face anti-spoofing," *IEEE Access*, 2025.
- [14] L. Li, Z. Xia, J. Wu, L. Yang, and H. Han, "Face presentation attack detection based on optical flow and texture analysis," *Journal of King Saud University-Computer and Information Sciences*, vol. 34, no. 4, pp. 1455–1467, 2022.
- [15] H. Xu, J. Zhang, J. Cai, H. Rezaatofighi, F. Yu, D. Tao, and A. Geiger, "Unifying flow, stereo and depth estimation," *IEEE Transactions on Pattern Analysis and Machine Intelligence*, vol. 45, no. 11, pp. 13 941–13 958, 2023.
- [16] S. Khan, T. H. M. Siddique, M. S. Ibrahim, A. J. Siddiqui, and K. Huang, "Spatio-temporal deep learning for improved face presentation attack detection," *Knowledge-Based Systems*, p. 113059, 2025.
- [17] T. H. M. Siddique, S. Khan, Z. Wang, and K. Huang, "Advspoofguard: Optimal transport driven robust face presentation attack detection system," *Knowledge-Based Systems*, p. 113759, 2025.
- [18] S. M. Ibrahim, M. S. Ibrahim, S. Khan, Y.-W. Ko, and J.-G. Lee, "Improving face presentation attack detection through deformable convolution and transfer learning," *IEEE Access*, 2025.
- [19] I. Chingovska, A. Anjos, and S. Marcel, "On the effectiveness of local binary patterns in face anti-spoofing," in *2012 BIOSIG-proceedings of the international conference of biometrics special interest group (BIOSIG)*. IEEE, 2012, pp. 1–7.
- [20] A. Costa-Pazo, S. Bhattacharjee, E. Vazquez-Fernandez, and S. Marcel, "The replay-mobile face presentation-attack database," in *2016 international conference of the Biometrics Special Interest Group (BIOSIG)*. IEEE, 2016, pp. 1–7.
- [21] H. Li, W. Li, H. Cao, S. Wang, F. Huang, and A. C. Kot, "Unsupervised domain adaptation for face anti-spoofing," *IEEE Transactions on Information Forensics and Security*, vol. 13, pp. 1794–1809, 2018. [Online]. Available: <https://api.semanticscholar.org/CorpusID:4624345>
- [22] Z. Boulkenafet, J. Komulainen, L. Li, X. Feng, and A. Hadid, "Oulunpu: A mobile face presentation attack database with real-world variations," in *2017 12th IEEE international conference on automatic face & gesture recognition (FG 2017)*. IEEE, 2017, pp. 612–618.
- [23] X. Guo, Y. Liu, A. Jain, and X. Liu, "Multi-domain learning for updating face anti-spoofing models," in *European conference on computer vision*. Springer, 2022, pp. 230–249.
- [24] X. Long, J. Zhang, and S. Shan, "Confidence aware learning for reliable face anti-spoofing," *IEEE Transactions on Information Forensics and Security*, 2025.
- [25] M. O. Allassafi, M. S. Ibrahim, I. Naseem, R. AlGhamdi, R. Alotaibi, F. A. Kateb, H. M. Oqaibi, A. A. Alshdadi, and S. A. Yusuf, "Fully supervised contrastive learning in latent space for face presentation attack detection," *Applied Intelligence*, vol. 53, no. 19, pp. 21 770–21 787, 2023.
- [26] V. D. Huszár and V. K. Adhikarla, "Securing phygital gameplay: Strategies for video-replay spoofing detection," *IEEE Access*, 2024.
- [27] X. Shu, H. Tang, and S. Huang, "Face spoofing detection based on chromatic ed-lbp texture feature," *Multimedia Systems*, vol. 27, no. 2, pp. 161–176, 2021.
- [28] N. Daniel and A. Anitha, "Texture and quality analysis for face spoofing detection," *Computers & Electrical Engineering*, vol. 94, p. 107293, 2021.
- [29] M. Alshaiqli, O. Elharrouss, S. Al-Maadeed, and A. Bouridane, "Face-fake-net: The deep learning method for image face anti-spoofing detection: Paper id 45," in *2021 9th European Workshop on Visual Information Processing (EUVIP)*. IEEE, 2021, pp. 1–6.
- [30] K. W. Lee, J. Y. Lim, K. M. Lim, and C. P. Lee, "Face presentation attack detection via ensemble learning algorithm," in *2023 IEEE 11th Conference on Systems, Process & Control (ICSPC)*. IEEE, 2023, pp. 101–106.
- [31] Z. Ning, W. Zhang, and J. Yang, "Face anti-spoofing based on 3d learnable convolutional operators," in *2024 36th Chinese Control and Decision Conference (CCDC)*. IEEE, 2024, pp. 4034–4040.